Operating Band Shifting of Resistor-Loaded Antenna-Based Absorber by Using Parasitic Element Concept

Zhekov, Stanislav Stefanov; Mei, Peng; Pedersen, Gert Frølund; Fan, Wei

Published in:
I E E E Transactions on Antennas and Propagation

DOI (link to publication from Publisher):
10.1109/TAP.2022.3161357

Publication date:
2022

Document Version
Accepted author manuscript, peer reviewed version

Operating Band Shifting of Resistor-Loaded Antenna-Based Absorber by Using Parasitic Element Concept

Stanislav Stefanov Zhekov, Peng Mei, Gert Frølund Pedersen, and Wei Fan

***Abstract*—The size of an electromagnetic (EM) absorber is a critical design parameter since it determines the operating frequency band. The realization of lower starting frequency requires enlargement of the absorber which often is not desired. In this communication, a technique for overcoming this problem in the case of an absorber, constructed of a resistor-loaded wideband bowtie antenna, is studied. The method is about placing parasitic elements around the antenna in order to change its input impedance and thus to realize large shifting of the operating band of both single- and dual-polarized absorbers. Without using parasitic elements large move of the operating band can only be achieved by a considerable increase in the absorber's size. However, the used method for absorption band shifting leads to shrinking of the bandwidth which means a compromise is to be made between these two parameters. For validation purposes, prototypes are fabricated and tested, and a good agreement between the simulation and measurement results is obtained.**

***Index Terms*—Electromagnetic absorber, operating band shifting, parasitic elements, resistor, wideband.**

I. Introduction

The electromagnetic absorber is a structure used to attenuate the signal impinging on it, meaning to reduce both the reflected from and transmitted through it part of that signal. Lately efforts toward the development of absorbers using periodic metal patterns have been devoted. Often, the absorber is required to operate over a wide frequency band. Different designs with wideband absorption have been proposed: 1) structures combining the resonances of multiple resonators [1], [2], 2) resistor-loaded structures [3]–[6], 3) structures using patterns made of resistive material [7], [8]; 4) structures employing magnetic materials [9]–[11]; and 5) structures employing combination of methods [12], [13]. A branch of the absorbers belonging to the second group is of interest in this communication. Specifically, we are focusing on absorbers designed by using a wideband dipole-like antenna the arms of which are connected through a lumped resistor (makes the structure lossy and thus the impinging wave is dissipated) [4].

The achievement of a well-operating absorber constructed by using conventional materials (e.g. carbon loaded foam) with a compact size is challenging. The lower frequency operation requires enlarging the absorber which might become too bulky. An advantage of structured absorbers is that they are smaller than the conventional ones. However, the shifting of the operating band of the structured absorbers towards lower frequency also requires increasing of their size [14]. Small anechoic chambers and cloaking technology, as two potential applications for these absorbers, might suffer from the size shortcoming since they need low-profile absorbers.

Absorbers with small unit cell have been presented in [1], [5], [7], [9]–[13]. Disadvantages of these structures are: need of having both empty and containing resonators unit cells (the sub-cells should be randomly distributed) [1]; convoluted structure containing multiple resistors (complex design) [5]; multi-layer structure (not desirable for many applications) using resistive surfaces (high cost) [7]; need of special magnetic material, meaning highly complex structure and technology [9]–[11]; multi-layer complex designs [12], [13] . A narrowband and complex (need of multiple lumped capacitors and through vertical interconnects), but thin, absorber has been shown in [15]. Loading with a capacitive structure (extra layer) to decrease the thickness of a narrowband filter based on frequency selective surface has been presented in [16]. We also use a passive way, which is cheap and robust, to achieve the miniaturization but the focus is on an absorber and there is no need to add an extra layer to the structure. Shifting of the operating band of a single-polarized bowtie antenna-based absorber by adding parasitic patches has been observed in our previous work [14]; this phenomenon is of interest for the realization of low-profile absorbers. However, this technique has only been briefly discussed since it has not been the main focus of that work. Moreover, the important case of a dual-polarized absorber has not been considered before.

In this communication, we present a novel framework to lower the operating band of an antenna-based absorber without increasing its size, as the band shifting is achieved by adding parasitic elements around the antenna. Thus, for the first time in this work a practical method capable to attain the goal of "miniaturizing" an absorber is introduced as well as its advantages and limitations are demonstrated: the dependence of the band shifting on the parasitic element; the achieved gain in the size of the absorber, i.e. lowering the starting frequency while keeping the same size; and the trade-off between the band shifting and achieved bandwidth. Both single- and dual-polarzied absorbers are considered. All numerical studies were performed by using CST microwave studio 2020.

II. Single-Polarized Absorber

A. Design of the Basic Absorber

The single-polarized absorber was designed by stepping on a wideband bowtie antenna. The unit cell is shown in Fig.

The authors are with the Department of Electronic Systems, Technical Faculty of IT and Design, Aalborg University, Aalborg, Denmark (e-mail: stz@es.aau.dk; mei@es.aau.dk; gfp@es.aau.dk; wfa@es.aau.dk)

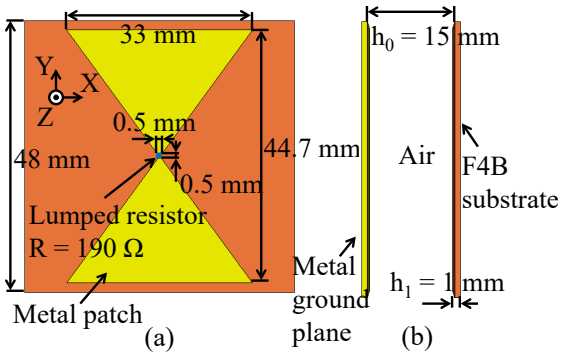

Fig. 1: Geometry of the basic wideband single-polarized absorber based on a bowtie antenna: (a) top view, and (b) side view.

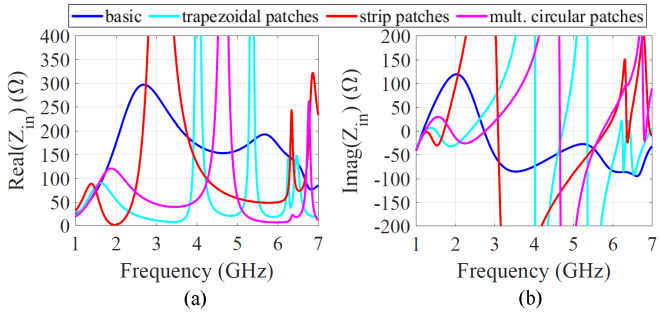

Fig. 2: Input impedance of the studied single-polarized absorbers: (a) real, and (b) imaginary part.

1; this structure is named "basic" throughout this section. The dimensions of the metal patches are selected so that to achieve wide absorption bandwidth for this unit cell. Lower operating band can be achieved by enlarging the patches but the bandwidth is narrower. The dielectric substrate (thickness h_1 = 1 mm) was made of F4B material (relative permittivity of 2.65 and loss tangent of 0.002). The copper (conductivity of 5.8x10^7 S/m), making the patches, had thickness of 0.035mm. On the back, a metal plate, separated from the substrate by an air layer with a height h_0 = 15 mm, was placed. The metal plate blocks the signal and thus the absorption coefficient can be calculated by using only the reflection coefficient. The two arms of the dipole were connected through a lumped resistor. The packaging of the resistors was 0.5 mm in both width and length (0402 package was used but the length was taken as 0.5 mm instead of 1 mm because the contacts/soldering pads were considered as part of the antenna arms).

The electric (E) field of the EM wave impinging the absorber was parallel to the y-axis. The input impedance of the absorber is presented in Fig. 2, while the reflection coefficient, when using a resistor with a value of $R = 190\ \Omega$, is presented in Fig. 3; see results for "basic". The value of the resistor was selected so that to maximize the frequency band for which the reflection coefficient is below -10 dB. The obtained absorption band ranges from 2 GHz to 6.5 GHz (106% bandwidth).

B. Operating Band Shifting

To study the possibility to move the absorption band towards lower frequency, several different parasitic elements placed around the arms of the bowtie antenna, were investigated; the

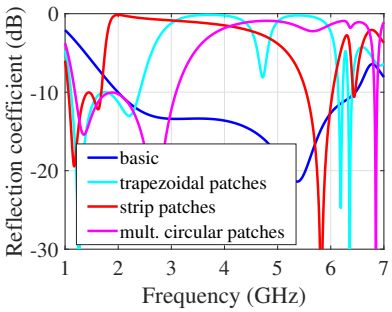

Fig. 3: Reflection coefficient of the studied single-polarized absorbers.

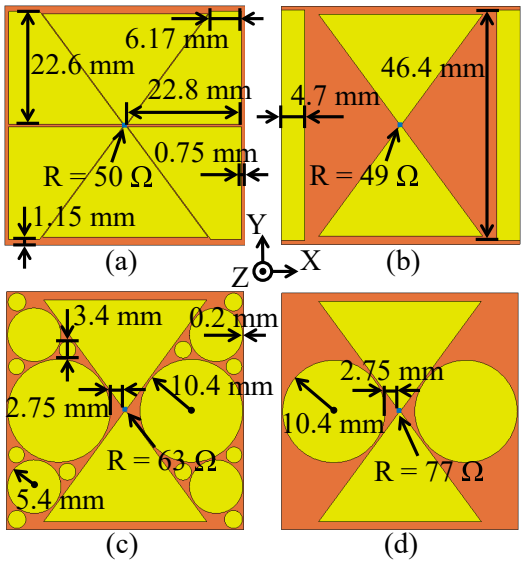

Fig. 4: Geometry of the studied single-polarized absorbers with parasitic elements around the bowtie antenna: (a) trapezoidal, (b) strip, (c) multiple circular, and (d) two circular parasitic patches.

geometry of the basic absorber was kept the same. The studied parasitic elements had shapes of: trapezoidal in Fig. 4(a) - this design is labeled as "trapezoidal patches" when presenting the results; strip in (b) - "strip patches"; and circular in both (c) - "circular patches" and (d) - "two circular patches".

The input impedance of the structures from Fig. 4(a)-(c) is shown in Fig. 2. A shift of the peak in the real part of the impedance towards lower frequencies, when parasitic patches are added, is observed. The parasitic elements introduce capacitive reactance and thus compensates partly the high peak inductive reactance appearing in the impedance of the basic design around 2 GHz. At low frequency, both real and imaginary parts of the impedance of the designs with parasitic elements show smaller absolute value as well as smaller variation compared to the basic design. Thus, this method for impedance loading enables operating at low frequency. However, at high frequency large change in the impedance is observed for the designs with parasitic elements.

To see the impact of the change in the input impedance on the reflection coefficient of the absorbers, resistors were added between the triangular patches, and the data are presented in Fig. 3. The values of the resistors (see Fig. 4) were selected to achieve the lowest working frequency while having

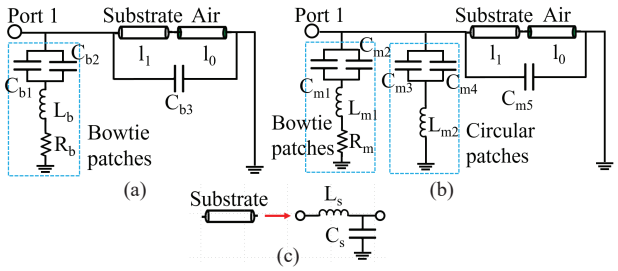

Fig. 5: Equivalent circuits of the absorbers: (a) basic design ($C_{b1} = 0.0765$ pF, $C_{b2} = 0.11$ pF, $C_{b3} = 0.03$ pF, $L_b = 10.02$ nH, and $R_b = 235\ \Omega$), and (b) design with multiple circular patches ($C_{m1} = 0.12$ pF, $C_{m2} = 0.255$ pF, $C_{m3} = 0.04$ pF, $C_{m4} = 0.01$ pF, $C_{m5} = 0.202$ pF, $L_{m1} = 18$ nH, $L_{m2} = 17.5$ nH, and $R_m = 200\ \Omega$). In (c) is shown that the substrate can be replaced with a combination of a series inductance and a shunt capacitance.

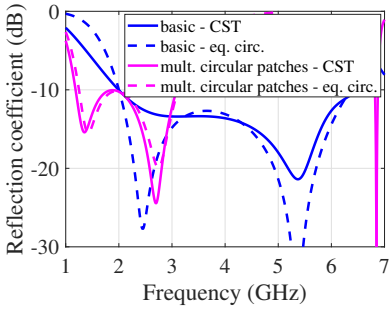

Fig. 6: Comparison between the reflection coefficients obtained by CST and by equivalent circuit ("eq. circ.") for the basic design and the one with multiple circular patches.

a continuous operating band. That is, if one tries to shift the operating frequency further to the left then the reflection coefficient will pass -10 dB level (at frequency between 1.5 and 2 GHz depending on which of the three studied designs is considered). A large shift in the position of the operating band is observed. For this unit cell (changes in the unit cell will lead to different results), the lowest starting frequency has the structure containing strip patches - 1.06 GHz (47% shifting of the lowest operating frequency - the basic design starts at 2 GHz) but has the smallest bandwidth - 45%. The design with multiple circular patches has the highest starting frequency of 1.19 GHz (41% shifting) but the widest operating band - 89%. Therefore, various designs and sizes of the parasitic elements can be used to change the position of the lowest operating frequency. In general, larger in size parasitic elements are needed to shift more the absorption band.

The equivalent circuits of the basic design (Fig. 1) and that of the design with multiple circular patches (Fig. 4(c)) are shown in Fig. 5. The capacitors are labeled with C_i while inductors with L_i. The model for the free-standing (when the substrate is not considered, i.e. removed): 1) bowtie patches consists of C_{b1} and L_b in the basic design; 2) bowtie patches consists of C_{m1} and L_{m1} and parasitic patches of C_{m3} and L_{m2} in the design with multiple circular patches. When the substrate is added, the circuits for the bowtie and parasitic patches need to be changed by introducing offset values - shunt capacitors C_{b2}, C_{m2}, and C_{m4}. The shunt capacitors C_{b3} and C_{m5} model the capacitance between the patches and the ground plane. The air layer and substrate are modeled as lossless transmission lines with electrical lengths of $l_0 = 2\pi f h_0/c$ and $l_1 = 2\pi f\sqrt{\epsilon_r h_1/c}$, respectively; c is the speed of light in vacuum; ϵ_r is the relative permittivity of the substrate. The use of transmission lines to model the air layer and substrate is a common technique [3], [17]. An electrically thin substrate (transmission line) can also be modeled with an equivalent circuit consisting of a series inductance ($L_s = \mu_0\mu_r h_1$) and a shunt capacitance ($C_s = \epsilon_0\epsilon_r h_1/2$) [17], as shown in Fig. 5(c); ϵ_0 is the permittivity of vacuum, while μ_0 and μ_r are the permeability of vacuum and the relative permeability of the dielectric material, respectively. The impedance of the grounded air layer can be expressed as $Z_a = jZ_0\tan\beta_0 h_0$, where $Z_0 = 337\ \Omega$ is the free space impedance and $\beta_0 = 2\pi/\lambda$ is the wavenumber. The addition of the parasitic patches: 1) changes C and L of the bowtie structure; 2) changes C between the top and bottom layer; and 3) adds their own C and L to the structure. The capacitance of the design with parasitic patches compensates more its inductance and thus reactance closer to 0 Ω is achieved compared to the reactance of the basic absorber at low frequency. This allows shifting of the operating band. The reflection coefficient obtained by CST matches well with that determined by the equivalent circuits for the two designs as presented in Fig. 6.

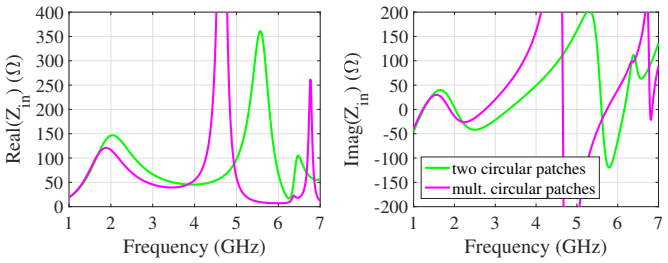

(a) (b)

Fig. 7: Input impedance of the single-polarized absorbers containing parasitic circular patches (see the designs in Fig. 4(c), (d)).

C. Relationship between the Band Shifting and the Bandwidth

Dependence between the degree of band shifting and the absorption bandwidth was observed. To illustrate this relationship, the designs in Fig. 4(c) and (d) are considered. Fig. 7 shows the input impedance of these two structures. The design with only two circular patches demonstrates a larger variation in both real and imaginary parts of the input impedance at low frequency. However, this design has a smaller increase in the magnitude of the input impedance at high frequency and this increase is moved to the right. The impact of the latter can be seen from the reflection coefficient shown in Fig. 8. The design with multiple circular patches has 6% lower starting frequency but 9% narrower operating band compared to the design with only two circular patches. In general, the lower the starting frequency the narrower the operating band.

D. Gain in the Height of the Absorber

It is of interest to see how much the absorber's height can be reduced, by using the proposed method, while keeping the

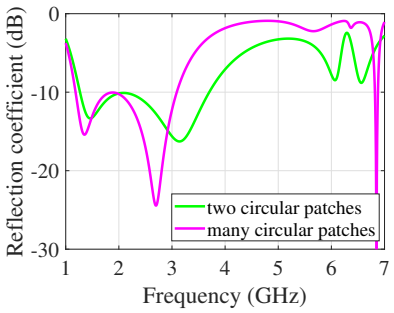

Fig. 8: Reflection coefficient of the single-polarized absorbers containing parasitic circular patches.

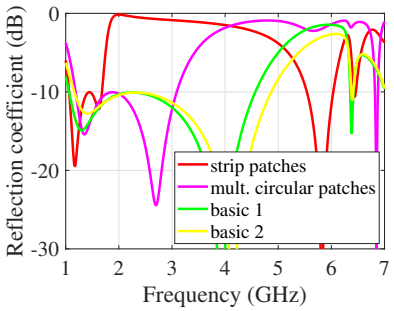

Fig. 9: Reflection coefficient of "strip patches", "mult. circular patches", "basic 1", and "basic 2" absorbers.

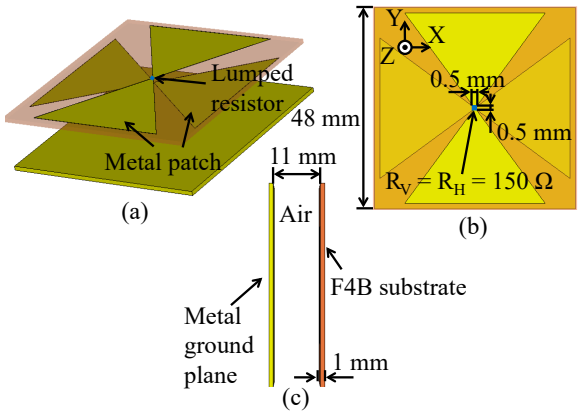

Fig. 10: Geometry of the primary dual-polarized absorber: (a) perspective, (b) top, and (c) side view. In (a) and (b) the substrate is made semitransparent for better visualization of the bottom layer.

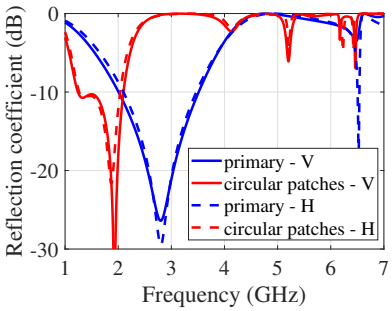

Fig. 11: Reflection coefficient of the primary dual-polarized absorber and the absorber with multiple circular patches.

same lowest operating frequency. For the basic design (lowest frequency of 2 GHz) the height of the air layer is 15 mm and this height needs to be enlarged to shift the lowest frequency to the left. Keeping all dimensions the same and only enlarging the height of the air layer of the basic structure, two designs were considered, with air layer of: 1) 23 mm (this design is named "basic 1"); and 2) 21 mm ("basic 2"). Fig. 9 shows the reflection coefficient of these two designs together with that for the design with strip and with multiple circular patches. Basic 1 (used resistor of 122 Ω) has starting frequency close to that for the design with strip patches, while the lowest frequency for basic 2 (resistor of 127 Ω) is close to that for the design with multiple circular patches. The total height of the basic absorber needs to be significantly enlarged to shift the operating band as much as in the case with the parasitic elements. That is, the gain in the absorber's height is large when parasitic elements are used. For this specific unit cell, 50% larger height is needed to reach the lowest frequency of the design with strip patches. However, the use of parasitic elements shrinks the bandwidth, i.e. this method is applicable when low-profile absorbers with low starting frequency are required and sacrifice of the bandwidth can be tolerated.

The starting frequency of the basic design can also be lowered by increasing the size of the triangular patches; further lowering requires also increase of the size of the unit cell. The reduction in the planar size of the unit cell, when parasitic elements are used, can be studied in the same way as that for the height. The use of larger triangles (with size close to that of the side of the unit cell) and adding small parasitic elements (less space in the unit cell due to the large triangles) in some cases might be less beneficial in terms of band shifting than using smaller triangles and larger parasitic elements.

III. Dual-Polarized Absorber

Often the absorber is required to operate for both linear polarizations and the presented method can be extended for this case. To demonstrate that, first, another bowtie antenna was printed on the backside of the substrate orthogonal to the top one. The unit cell of the dual-polarized absorber (labeled with "primary") is presented in Fig. 10. The dimensions of the triangles and the planar size of the unit cell are the same as those for the single-polarized case (Fig. 1); keeping of the same dimension was done for simplicity, although thus obtained absorber is not optimal neither in terms of bandwidth or starting frequency. The height of the air layer was 11 mm. The triangular patches of each bowtie antenna were connected through resistor $R_V = R_H = 150\ \Omega$ (these were the optimal resistors), as R_V is the label for the resistor for the top bowtie antenna and R_H for the bottom one. The reflection coefficient of the two absorbers is presented in Fig. 11; the data are labeled with "primary". In the rest of the communication, with V are labeled the results for the top bowtie absorber, while with H those for the bottom one. As one can see from Fig. 11, the absorption for both polarizations is similar. The thickness of the air layer was selected so that the lowest operating frequency is around 2 GHz as in the single-polarized case.

To demonstrate the possibility for shifting of the operating band towards lower frequency for the dual-polarized absorber,

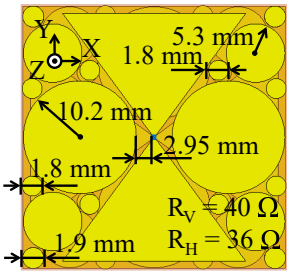

Fig. 12: Top view of the dual-polarized absorber with multiple circular patches around the two bowtie antennas.

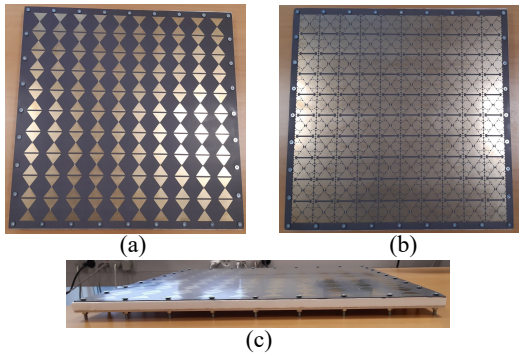

Fig. 13: Photographs of the manufactured prototypes: (a) primary absorber, (b) absorber with multiple circular patches. Top view is presented in (a) and (b), while in (c) side view.

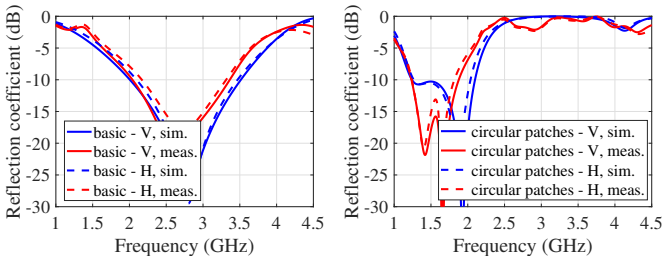

Fig. 14: Measured (labeled with "meas.") and simulated (labeled with "sim.") reflection coefficient of: (a) primary dual-polarized absorber, and (b) dual-polarized absorber containing circular patches.

an example, where multiple circular patches were added, was considered. The design (top and bottom layers are the same just inverted at 90°), together with the dimensions of the parasitic elements, is shown in Fig. 12. The used resistors for this absorber were $R_V = 40\ \Omega$ (top dipole) and $R_H = 36\ \Omega$ (bottom dipole). The reflection coefficient is presented in Fig. 12; the results are labeled with "circular patches". As one can see a shift of 38% in the lowest frequency for this specific design is achieved (larger shifting can be achieved as discussed below). The shrinking of the bandwidth is not so high in this case - the primary design has 55% while the design with parasitic elements 51% bandwidth. It should be mentioned that, for this geometry of the absorber, a design with parasitic trapezoidal patches (they provide larger band shifting than circular one) was also studied (not shown). In this case, shifting of the lowest operating frequency of 56% was achieved but the bandwidth of the structure was of 17%.

IV. Experimental Verification

To confirm the simulation results, both dual-polarized absorbers from Fig. 10 and Fig. 12 were fabricated and photographs of the prototypes are given in Fig. 13(a) and (b), respectively. The air gap was ensured by placing in between the substrate and the metal ground plane a layer of styrofoam (its dielectric properties are very close to those of air), as shown in Fig. 13(c). To assemble the structure as a whole, screws were used for attaching the substrate, styrofoam, and ground plane. The setup for measuring the reflection coefficient of the absorber included one transmitting and one receiving antenna, connected to a network analyzer. The study was performed in an anechoic chamber, and consisted of measuring S_{21} for metal plate and that for the absorber. The reflection coefficient was calculated by taking the difference between the results from the two measurements in dB.

The simulated and measured reflection coefficients for each polarization for the primary design and the design containing multiple circular patches are presented in Fig. 14. The measurement and simulation results match, although the measured absorbtion bandwidth is 43%, while the simulated is 51%. The reflection coefficient of the absorbers at 30° angle of incidence for transverse electric (TE) and transverse magnetic (TM) polarization of the EM wave were simulated and measured, and the results are presented in Fig. 15. According to the measurement results, the absorption bandwidth is acceptable when the angle of incidence is up to 30° (the worst case is for TE polarization for an angle of incidence of 30°). The simulation showed that at 15° angle of incidence the performance is good (not shown), but it deteriorates at 30°.

Two other advanced dual-polarized absorbers were developed, for the sake of the comparison below, as shown in Fig. 16(a), (b); both have thickness of 12 mm; the absorber in Fig. 16(a), labeled as "trap.", has the same planar size of the unit cell as the "primary" one, while the planar size of the absorber in Fig. 16(b), labeled as "sm. trap.", is smaller. The reflection coefficient for these two absorbers is given in Fig. 16(c); their primary designs have starting frequency around 2 GHz. The "trap." has very low starting frequency (0.76 GHz).

Table I (with "circ." is labeled the design in Fig. 12) presents comparison between performance of dual-polarized

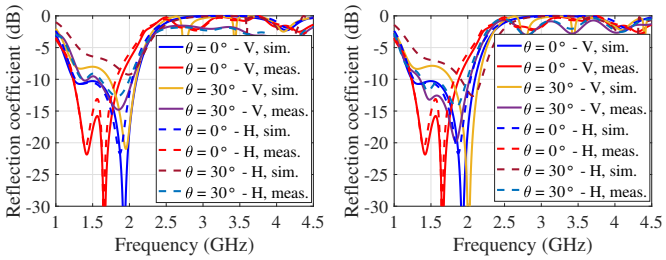

Fig. 15: Measured and simulated reflection coefficient of dual-polarized absorber containing multiple circular patches at 30° angle of incidence for: (a) TE, and (b) TM polarization of the EM wave.

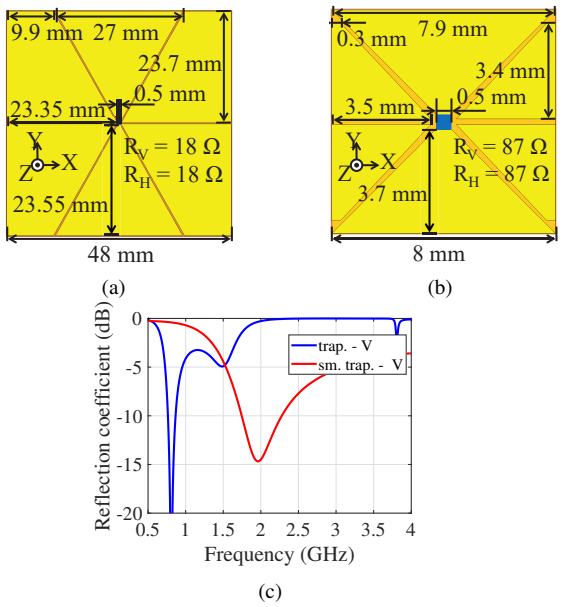

Fig. 16: Dual-polarized absorbers with trapezoidal parasitic elements: (a) labeled as "trap." , (b) labeled as "sm. trap."; the pictures in (a) and (b) are scaled. Reflection coefficient of the vertical (top) absorber for each structure is shown in (c).

absorbers. All designs in the table are either dual-polarized or completely polarization insensitive. The use of multiple layers makes the structure complicated (especially complex are [12], [13]), but allows wide bandwidth and good angle stability. Small thickness can be achieved by using resonating structures, as in [1], but the planar size of the unit cell (contains two different sub-cells) is large. By using multiple resistors, small unit cell [5], [10] and wide bandwidth (see [3], [6]) can be achieved, but this increases the price and makes the design complicated (in [5] is also used complex convoluted structure while in [10] magnetic material). The use of resistive layers (costly technology) provides wide bandwidth, but the unit cell is large [7], [8]. The use of special magnetic material allows realization of compact unit cell with large bandwidth, but the manufacturing technology is more complicated and expensive than conventional one [9]–[11]. The design "trap." has one of the smallest electrical thicknesses (and small volume compared to the designs with similar thickness) while the unit cell of design "sm. trap." has the smallest volume. Therefore, by the proposed method can be achieve small thickness or small side of the until cell. An advantage of the proposed method is that it is conventional and simple, the position of the operating band can be easily controlled through the size and shape of the parasitic elements and cheap (only two resistors are needed). The main disadvantage is that the absorber has relatively narrow operating bandwidth, especially when the parasitic elements are added and large band shifting is desired. By using more complicated designs, as those, in the literature wider bandwidth can be realized but the unit cell is larger.

V. Conclusion

A general method for shifting the operating band of an absorber, based on a resistor-loaded bowtie antenna, towards lower frequency has been discussed in this communication. The idea is to place around the antenna's arms parasitic elements and thus to change the structure's input impedance. If parasitic elements are not used then the shifting of the absorption band requires increase in the size of the absorber. Unfortunately, the band shifting by using parasitic elements leads to shrinking of the bandwidth. The presented method is helpful for applications, such as stealth technology and small anechoic chamber, where the size of the absorber is a critical design parameter.

TABLE I: Comparison between the dual-polarized absorbers "circ.", "trap.", and "sm. trap." with those available in the literature, in terms of size "X x Y x Z" and volume of the unit cells (unit: λ_{max}^3, where λ_{max} is the wavelength corresponding to the lowest operating frequency for reflection level of -10 dB), bandwidth "BW", fractional bandwidth "FBW", angle stability "AS", and the number of layers "No. lay." building the absorber. For "circ." for "BW" and "FBW" are given both measurement and simulation results.

Ref.	X x Y x Z Volume (λ_{max}^3)	BW (GHz)	FBW (%)	AS (°)	No. lay.
[1]	0.480 x 0.480 x 0.034 0.0078	16-33	69	<30	1
[5]	0.057 x 0.057 x 0.062 0.000201	0.86-0.96	11	<30	1
[6]	0.240 x 0.240 x 0.079 0.0046	5.3-11.2	70.7	< 30	1
[7]	0.071 x 0.071 x 0.089 0.000449	1.07-9.5	159	< 30	2
[8]	0.285 x 0.285 x 0.071 0.0058	10.7–29	92	<30	1
[9]	0.125 x 0.125 x 0.031 0.000484	4-15	115	<20	1
[10]	0.200 x 0.200 x 0.030 0.0012	4-18	127	<30	2
[11]	0.053 x 0.053 x 0.084 0.000236	1.05 – 2.7	88	<45	2
[12]	0.062 x 0.062 x 0.142 0.000546	3.7-17.2	129	<60	7
[13]	0.093 x 0.093 x 0.092 0.000796	1.85-19.2	164	<30	2
[18]	0.220 x 0.220 x 0.083 0.0040	4.8–11.1	90	<40	2
circ.	0.114 x 0.114 x 0.049 0.000637	1.23-1.9 (1.24-2.1)	43 (51)	<30 <30	1
trap.	0.121 x 0.121 x 0.030 0.000439	0.76-0.87	14	<30	1
sm. trap.	0.046 x 0.046 x 0.069 0.000146	1.74-2.28	27	<30	1

References

[1] M. Tran, V. Pham, T. Ho, T. T. Nguyen, H. T. Do, X. K. Bui, S. T. Bui, D. T. Le, T. L. Pham, and D. L. Vu, "Broadband microwave coding metamaterial absorbers," *Sci. Rep.*, vol. 10, 2020.

[2] Y. Cheng, Y. Nie, and R. Gong, "Metamaterial absorber and extending absorbance bandwidth based on multi-cross resonators," *Appl. Phys. B*, vol. 111, no. 3, pp. 483–488, 2013.

[3] Y. Shang, Z. Shen, and S. Xiao, "On the design of single-layer circuit analog absorber using double-square-loop array," *IEEE Trans. Antennas Propag.*, vol. 61, no. 12, pp. 6022–6029, 2013.

[4] X. Q. Lin, P. Mei, P. C. Zhang, Z. Z. D. Chen, and Y. Fan, "Development of a resistor-loaded ultrawideband absorber with antenna reciprocity," *IEEE Trans. Antennas Propag.*, vol. 64, no. 11, pp. 4910–4913, 2016.

[5] W. Zuo, Y. Yang, X. He, D. Zhan, and Q. Zhang, "A miniaturized metamaterial absorber for ultrahigh-frequency RFID system," *IEEE Antennas Wireless Propag. Lett.*, vol. 16, pp. 329–332, 2017.

[6] D. Kundu, A. Mohan, and A. Chakrabarty, "Single-layer wideband microwave absorber using array of crossed dipoles," *IEEE Antennas Wireless Propag. Lett.*, vol. 15, pp. 1589–1592, 2016.

[7] M. I. Hossain, N. Nguyen-Trong, K. H. Sayidmarie, and A. M. Abbosh, "Equivalent circuit design method for wideband nonmagnetic absorbers at low microwave frequencies," *IEEE Trans. Antennas Propag.*, vol. 68, no. 12, pp. 8215–8220, 2020.

[8] M. Li, S. Xiao, Y.-Y. Bai, and B.-Z. Wang, "An ultrathin and broadband radar absorber using resistive fss," *IEEE Antennas Wireless Propag. Lett.*, vol. 11, pp. 748–751, 2012.

[9] T. Deng, Z.-W. Li, and Z. N. Chen, "Ultrathin broadband absorber using frequency-selective surface and frequency-dispersive magnetic materials," *IEEE Trans. Antennas Propag.*, vol. 65, no. 11, pp. 5886–5894, 2017.

[10] W. Yuan, Q. Chen, Y. Xu, H. Xu, S. Bie, and J. Jiang, "Broadband microwave absorption properties of ultrathin composites containing edge-split square-loop fss embedded in magnetic sheets," *IEEE Antennas Wireless Propag. Lett.*, vol. 16, pp. 278–281, 2017.

[11] Y. N. Kazantsev, A. V. Lopatin, N. E. Kazantseva, A. D. Shatrov, V. P. Mal'tsev, J. Vilcáková, and P. Sáha, "Broadening of operating frequency band of magnetic-type radio absorbers by fss incorporation," *IEEE Trans. Antennas Propag.*, vol. 58, no. 4, pp. 1227–1235, 2010.

[12] X. Begaud, A. C. Lepage, S. Varault, M. Soiron, and A. Barka, "Ultra-wideband and wide-angle microwave metamaterial absorber," *Materials*, vol. 11, no. 10, 2018.

[13] L. Zhou and Z. Shen, "Absorptive coding metasurface with ultrawideband backscattering reduction," *IEEE Antennas Wireless Propag. Lett.*, vol. 19, no. 7, pp. 1201–1205, 2020.

[14] P. Mei, S. Zhang, X. Q. Lin, and G. F. Pedersen, "Design of an absorptive fabry–perot polarizer and its application," *IEEE Antennas Wireless Propag. Lett.*, vol. 18, no. 7, pp. 1352–1356, 2019.

[15] B. X. Khuyen, B. S. Tung, Y. J. Yoo, Y. J. Kim, K. W. Kim, L.-Y. Chen, V. D. Lam, and Y. P. Lee, "Miniaturization for ultrathin metamaterial perfect absorber in the VHF band," *Sci. Rep.*, vol. 7, 2017.

[16] P.-C. Zhao, Z.-Y. Zong, W. Wu, B. Li, and D.-G. Fang, "Miniaturized-element bandpass fss by loading capacitive structures," *IEEE Trans. Antennas Propag.*, vol. 67, no. 5, pp. 3539–3544, 2019.

[17] A. Ebrahimi, Z. Shen, W. Withayachumnankul, S. F. Al-Sarawi, and D. Abbott, "Varactor-tunable second-order bandpass frequency-selective surface with embedded bias network," *IEEE Trans. Antennas Propag.*, vol. 64, no. 5, pp. 1672–1680, 2016.

[18] T. Beeharry, R. Yahiaoui, K. Selemani, and H. H. Ouslimani, "A dual layer broadband radar absorber to minimize electromagnetic interference in radomes," *Sci. Rep.*, vol. 8, 2018.